第 26 卷第 12 期 无 机 化 学 学 报 Vol.26 No.12
2010 年 12 月 CHINESE JOURNAL OF INORGANIC CHEMISTRY 2289-2298

研究简报

钾锰氧化物:电化学控制合成及其电容器性质

冯良东[1,2] 石建军[1] 姜立萍*,[1] 朱俊杰[1]
([1]生命分析化学教育部重点实验室,南京大学化学化工学院,南京 210093)
([2]江苏省凹土资源利用重点实验室,淮阴工学院化工系,淮安 223003)

关键词:钾锰氧化物;阴极沉积;形貌;电容器
中图分类号:O611.62 **文献标识码**:A **文章编号**:1001-4861(2010)12-2289-10

Potassium Manganese Oxides: Electrochemically Controlled Synthesis and Capacitor Properties

FENG Liang-Dong[1,2] SHI Jian-Jun[1] JIANG Li-Ping*,[1] ZHU Jun-Jie[1]
([1]*Key Laboratory of Analytical Chemistry for Life Science (MOE), School of Chemistry and Chemical Engineering, Nanjing University, Nanjing* 210093)
([2]*Key Laboratory for Palygorskite Science and Applied Technology of Jiangsu Province, Department of Chemical Engineering, Huaiyin Institute of Technology, Huaian, Jiangsu* 223003)

Abstract: Potassium manganese oxides were prepared by cathodic deposition from aqueous $KMnO_4$ solution on an indium tin oxide slide. The products were characterized by XRD, XPS and SEM techniques. The as-prepared products were potassium manganese oxides with different manganese valence states. The component, morphology and size of the products could be controlled through adjusting the preparation parameters such as deposition potential, deposition time and acidity of the electrolyte. The results show that the deposition of potassium manganese oxide from aqueous $KMnO_4$ is a pH value dependent procedure. Due to the facilitating of intercalation and deintercalation of cations, the specific capacitance of the products deposited for 500 s is higher than that of 3 000 and 6 000 s. At a scan rate of 2 $mV\cdot s^{-1}$ in 0.2 $mol\cdot L^{-1}$ K_2SO_4 aqueous electrolyte, the specific capacitances of products are 119.4, 99.5 and 109.0 $F\cdot g^{-1}$ corresponding to the deposition time of 500, 3 000 and 6 000 s, respectively. Electrochemical experiments indicate that the reversibility and performance of these potassium manganese oxides are also changed with the deposition time.

Key words: potassium manganese oxide; cathodic deposition; morphology; capacitor

0 Introduction

Due to their excellent electrochemical properties, metal oxides such as RuO_2 and MnO_2 have shown high performance as electrode material in supercapacitors[1-4]. Although ruthenium oxide has the largest specific capacitance (SC) value of 2 200 $F\cdot g^{-1}$ and excellent reversibility, the high cost, toxic nature and the use of a

收稿日期:2010-07-30。收修改稿日期:2010-09-25。
国家自然科学基金(No.20635020,20821063,20605011)、江苏省自然科学基金(No.BK2008196)及江苏省“青蓝工程”资助项目。
*通讯联系人。E-mail:jianglp@nju.edu.cn
第一作者:冯良东,男,41 岁,博士;研究方向:材料电化学合成。

strong acidic electrolyte inhibit its commercial application. There have been increasing interests in finding alternatives to ruthenium oxide as advanced electrode materials. As a potential capacitor material, manganese oxide materials have shown excellent capacitive characteristics with high theoretical SC value (about 1 370 $F \cdot g^{-1}$) and are in abundance as well as non-toxic[3,5-7]. Therefore, a lot of efforts have been devoted to their capacitive characteristics.

The preparation techniques of manganese oxides for capacitor include electrochemical deposition, chemical co-precipitation[8-16], hydrothermal synthesis[17-20], sol-gel processes[21-25]. Electrochemical deposition technique is advantageous, because the mass, thickness, and morphology can be easily controlled by simply adjusting the electrochemical depositing parameters such as the component, acidity and temperature of the electrolyte. In addition, metal oxide films synthesized by electrochemical deposition are more likely to be nanostructured. The nanostructure of manganese oxide is especially important for the development of electrochemical capacitors. It has been shown that the SC of manganese oxides is influenced by some factors such as shape and crystal structure of the product, chemical composition, valence state of manganese, and surface area.

Previous electrochemical preparations were focused on anodic deposition of manganese oxides[26-30]. The anodic deposition variables such as current density, pH value, composition and temperature of plating bath were found to be the key factors influencing the SC of manganese oxide[28]. The deposits prepared by the anodic deposition were amorphous at annealing temperatures below 400 ℃ or contained poorly crystalline structure[4,26-27]. The mean oxidation state of Mn increased with increasing annealing temperature. The SC of manganese oxides deposited by anodic deposition decreased with increasing film thickness[30]. Besides the ability to avoid anodic dissolution of metallic substrates, cathodic deposition can also co-deposit various oxides and metals, and modify the composition, conductivity and electrochemical performance of the obtained products. Since the pioneering work of Zhitomirsky et al., there have some studies on the cathodic deposition of manganese oxides[31-42]. For example, birnessite manganese oxide films named as $K_xMnO_{2+y}(H_2O)_z$ has been prepared by galvanostatic pulse and reverse pulse deposition through cathodic reduction of $KMnO_4$ solutions, and the deposits microstructure can be varied by altering the deposition conditions[38]. Although the electrochemical capacitor properties of manganese dioxides have been extensively studied, the influence of fabrication parameters such as applied potential, deposition time and the acidity of the electrolytes on the component, morphology and size of the prepared products have not been elucidated clearly, and there have less reports on the deposition mechanism of cathodic deposition of manganese dioxides[41-42].

In this work, potassium manganese oxides with controllable size and shape were deposited by cathodic reduction of MnO_4^- ions at room temperature. The crystalline structure, surface morphology, component and chemical environment of the products were characterized with XRD, SEM and XPS techniques. The influence of deposition conditions on the component, morphologies and size of the products were examined. The capacitor properties of the potassium manganese oxides with different components, morphologies and sizes were studied by techniques of cyclic voltammetry (CV) and chronopotentiometry (CP).

1 Experimental

Analytical grade of potassium permanganate ($KMnO_4$), potassium nitrate (KNO_3), potassium sulfate (K_2SO_4) and other chemicals were purchased from Shanghai Chemical Reagent Co. All reagents were used without further purification, and distilled water was used throughout.

The potassium manganese oxides were synthesized by amperometric method. The deposition was carried out on a CHI 660C electrochemical workstation (Chenhua, Shanghai, China) at room temperature. A traditional three-electrode configuration was used with an indium tin oxide (ITO) slide as the working electrode. A platinum wire and a saturated calomel electrode (SCE) were served as counter electrode and reference electrode, respectively. All potentials given

below were relative to the SCE. In a typical procedure, the ITO electrode was immersed into the mixture containing 10.0 mmol·L^{-1} $KMnO_4$ and 0.1 mol·L^{-1} KNO_3 with different acidity, the potential was kept at a certain value for given times. Then, the ITO electrode was washed with doubly distilled water to remove the adsorbed salts. The ITO slide with deposited products was dried in a desiccator for XRD, SEM and electrochemical measurements. For XPS measurements, the electrodeposited potassium manganese oxides were scraped from the ITO slide by a stainless steel knife.

Powder XRD measurement was performed on a Shimadzu XD-3A X-ray diffractometer at a scanning rate of 4°·min^{-1} in the 2θ range from 10° to 80°, with graphite monochromatized Cu $K\alpha$ radiation (λ=0.154 18 nm). The XPS spectra were recorded on an ESCALAB MK Ⅱ X-ray photoelectron spectrometer by using nonmonochromatized Al $K\alpha$ X-ray as the excitation source and choosing C1*s* (284.6 eV) as the reference line. The SEM images were carried out on an S-3000 N (Hitachi, Japan) scanning electron microscope operating at 20 kV.

CV studies were performed within a potential range of 0~1.0 V with varying potential scan rates in a 0.2 mol·L^{-1} K_2SO_4 aqueous electrolyte. In the CP measurements, a current density of 0.5 A·g^{-1} was used to investigate the capacitor performance.

2 Results and discussion

2.1 XRD analysis

Fig.1 shows XRD patterns of potassium manganese oxides deposited in 10.0 mmol·L^{-1} $KMnO_4$ solutions at −0.6 V for different times. The changes in the component of the deposits are clearly noticed in the XRD patterns. The XRD pattern of the film deposited for 200 s (curve a) shows that the component of the film is a mixture of cryptomelane-type potassium manganese oxide ($K_{2-x}Mn_8O_{16}$, PDF No.44-1386) and birnessite-type potassium manganese oxide ($K_{0.46}Mn_2O_4$ $(H_2O)_{1.4}$, PDF No.80-1098). The diffraction peaks at 2θ=12.5° and 25.2° splitting into two or more broad peaks suggest that the product is a mixture of poorly crystallized microdomains with slightly different cell parameters[43]. The ratio of the strongest peaks integral intensity areas shows that the content of birnessite-type potassium manganese oxide is less. When the deposi-tion time reaches 4 000 s, the intensity of birnessite-type potassium manganese oxide peaks become stronger, implying that the content of birnessite -type potassium manganese oxide increases with the deposition time as shown in b. If the deposition time extends to 9 000 s, the product is mainly composed of birnessite-type potassium manganese oxide as displayed in c. The XRD results indicate that the component of the products was varying with deposition time.

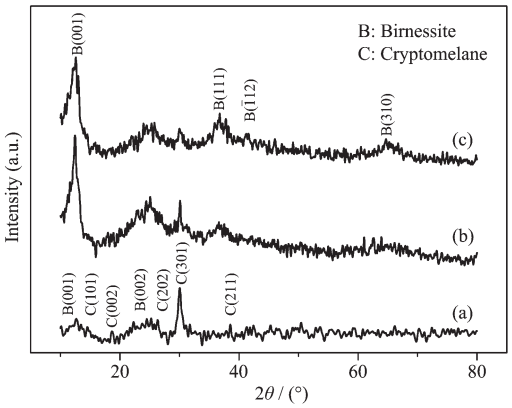

(a) 200, (b) 4 000, (c) 9 000 s

Fig.1　XRD patterns of samples deposited at −0.6 V for different times

2.2 XPS studies

The XPS spectra of the products deposited at −0.6 V for 9 000 s are shown in Fig.2. Fig.2a shows the wide-scan XPS spectrum of the potassium manganese oxides. The only detectable peaks of K, Mn, O and the added reference C are observed, which confirms that the product is a compound of potassium manganese oxide.

The high-resolution XPS spectra of Mn3*s*, Mn2*p*, and O1*s* are shown in Fig.2b, 2c and 2d, respectively. Due to the parallel spin coupling of the 3*s* electron with the 3*d* electron during the photoelectron ejection, Mn3*s* core level spectrum usually shows a peak splitting and a doublet[44]. The magnitude of the splitting energy of Mn3*s* photoelectron peaks (ΔE) is known to increase approximately linearly as the Mn oxidation state (n) decreases: ΔE=7.88~0.85n[45]. As reported in Fig.2b, the Mn3*s* splitting energy for the product is about 5.17 eV, and the calculated average oxidation states of

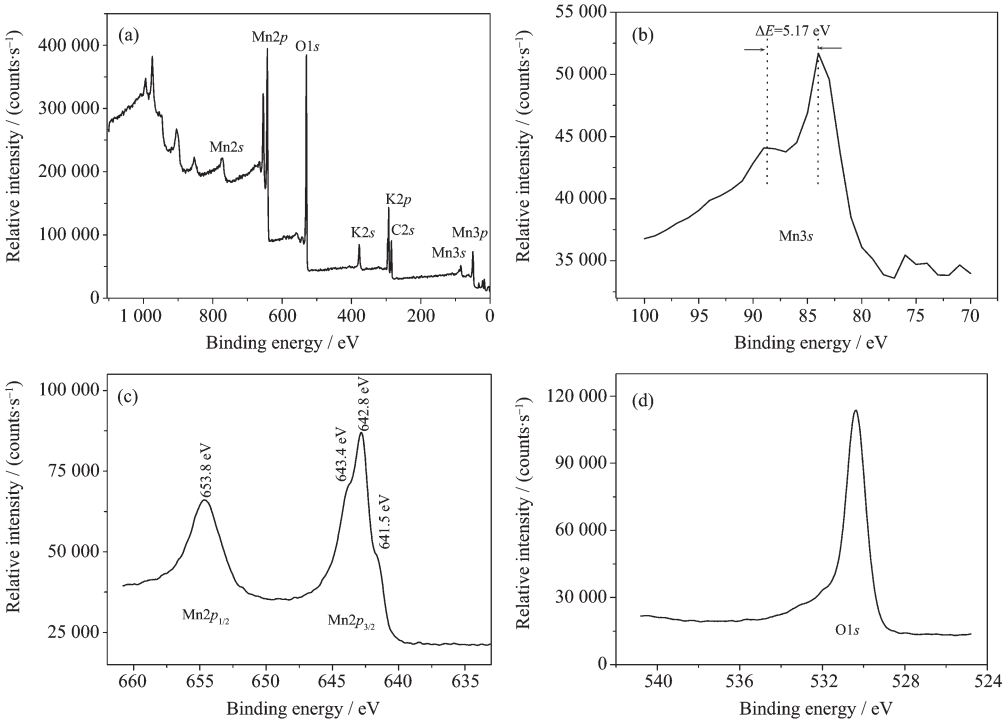

Fig.2 XPS spectra of the as-prepared sample: (a) survey spectrum, (b) high-resolution spectrum of Mn3*s*, (c) high-resolution spectrum of Mn2$p_{1/2}$ and Mn2$p_{3/2}$, and (d) high-resolution spectrum of O1*s*

surface Mn atoms is about 3.2. In Fig.2c, the Mn2$p_{3/2}$ and Mn2$p_{1/2}$ transitions are centered at 642.6 and 653.8 eV, respectively. The Mn2$p_{3/2}$ spectrum shows two peaks with maximum at 642.8 and 643.9 eV, and having spin energy separation of 11.0 and 9.9 eV with the satellite Mn2$p_{1/2}$ peak. The spin energy separations are consistent with the reported data for Mn(Ⅲ) and Mn(Ⅳ) oxides[46], which means the product contains different valence states of manganese. Existence of the Mn-oxide phases is also reflected in the O1*s* core level spectrum shown in Fig.2d, the peak at 530.3 eV can be ascribed to the oxide peak (Mn-O-Mn)[44], and the peaks of Mn-O-H (530.5~531.5 eV) and water molecule (531.8~532.8 eV) are invisible[26,44,47-49]. Thus, it is clear that the obtained product in the present work is a potassium manganese oxide with different valence states of manganese.

2.3 SEM studies

In the experiments, when an ITO electrode was placed in a solution with 10.0 mmol·L^{-1} $KMnO_4$ and 0.1 mol·L^{-1} KNO_3 and was deposited at −0.6 V for different times, different morphologies of potassium manganese oxides such as thin film, nano-/micro- sized particles and microfiber assemblies are shown in Fig.3. The morphology of the products deposited for 200 s is mainly three-dimensional networks formed by nanofibers and less particles with diameter of about 500 nm on the networks surface as shown in Fig.3a. After depositing for 500 s, there are plenty of particles with diameter of about 1.0~2.0 μm in the products assembled with tiny particles of about 50~100 nm as depicted in Fig.3b. If the deposition time is extended to 3 000 s, the products are developed to erective microfibers with length of about 3.0 μm and diameter of 0.8~2.0 μm, and there are also plenty of tiny particles on the surface and less particles on the tip of the microfibers as shown in Fig.3c. Further extending the deposition time to 6 000 s, there are plenty of tiny particles deposited on the microfibers tips as shown in Fig.3d. The products become into individual fragment at 9 000 s (Fig.3e). Through careful observation, one can see that the individual fragment is composed of three layers, a compact film with thickness of about 50 nm on the bottom (as marked in Fig.3e), bundles of microfibers in the middle, and aggregated microparticles on the top of the microfibers.

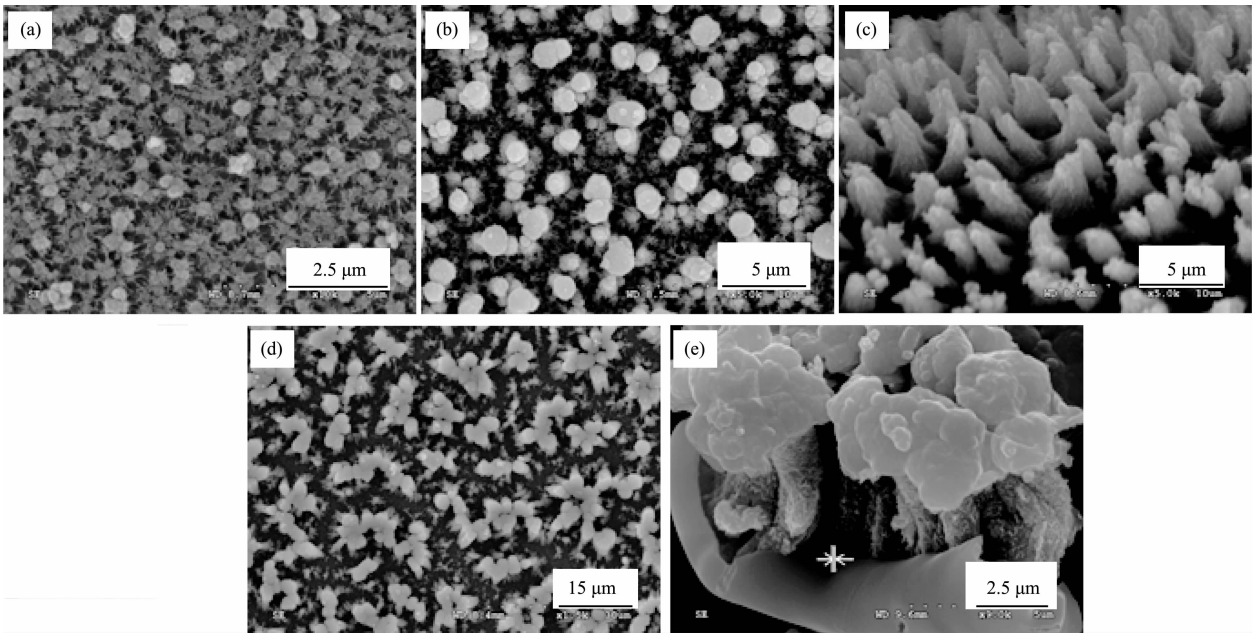

(a) 200, (b) 500, (c) 3 000, (d) 6 000 and (e) 9 000 s

Fig.3　SEM images of the as-prepared products deposited at −0.6 V for different times

The changing of the products morphology and component with deposition time can be explained as follows. In a solution of 10.0 mmol·L^{-1} $KMnO_4$ and 0.1 mol·L^{-1} KNO_3, when a potential of −0.6 V is applied, the MnO_4^- ions is mainly reduced to Mn(Ⅳ) in the form of cryptomelane-type with a small amount of birnessite-type potassium manganese oxide. Increasing the deposition time, the concentration of H^+ ions in the electrolyte decreases with the consuming of MnO_4^- ions in the reduction procedure, thereby, the as-prepared product is a mixture of cryptomelane-type and birnessite-type potassium manganese oxide. Further increase in deposition time will result in much less H^+ ions in the electrolyte, and the birnessite-type potassium manganese oxide is the dominating component in the products for longer deposition time such as 6 000 and 9 000 s. The current-time curves recorded in the preparing procedures shown in Fig.4 indicate the pH value dependent formation procedures of the products, i.e., fromation of a thin compacted film to assembling microfibers and to aggregate microparticles in the end, corresponding to the three parts shown in Fig.3e.

In order to further investigate the effect of electrolytes acidity on the morphologies and

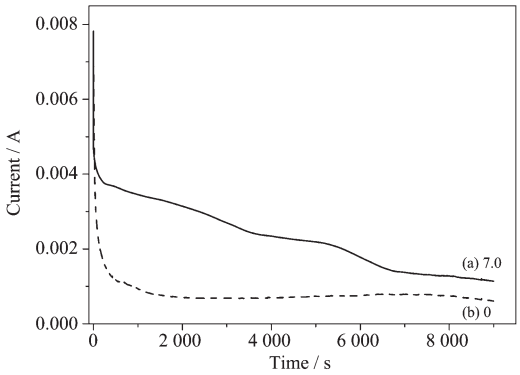

Fig.4　Current-time curves of the preparing procedures at −0.6 V for 9 000 s in different initial pH value electrolytes

microstructures of the products, the solutions with different pH values were adopted to prepare potassium manganese oxides. The products were deposited at −0.6 V for 1 000 s. If the initial pH value of the solutions is controlled to be 0, the prepared products are composed of spherical aggregates of nanoparticles without clear boundary, and the diameter of the spheres is 1.0 to 1.5 μm. Carefully examination reveals that the particles consist of crosslinked three-dimensional nanofibers with a few tens of nano-meters in size, as shown in Fig.5a. Fig.5b shows the morphology of the products deposited at pH value of 3.0, the deposits consist of small needle

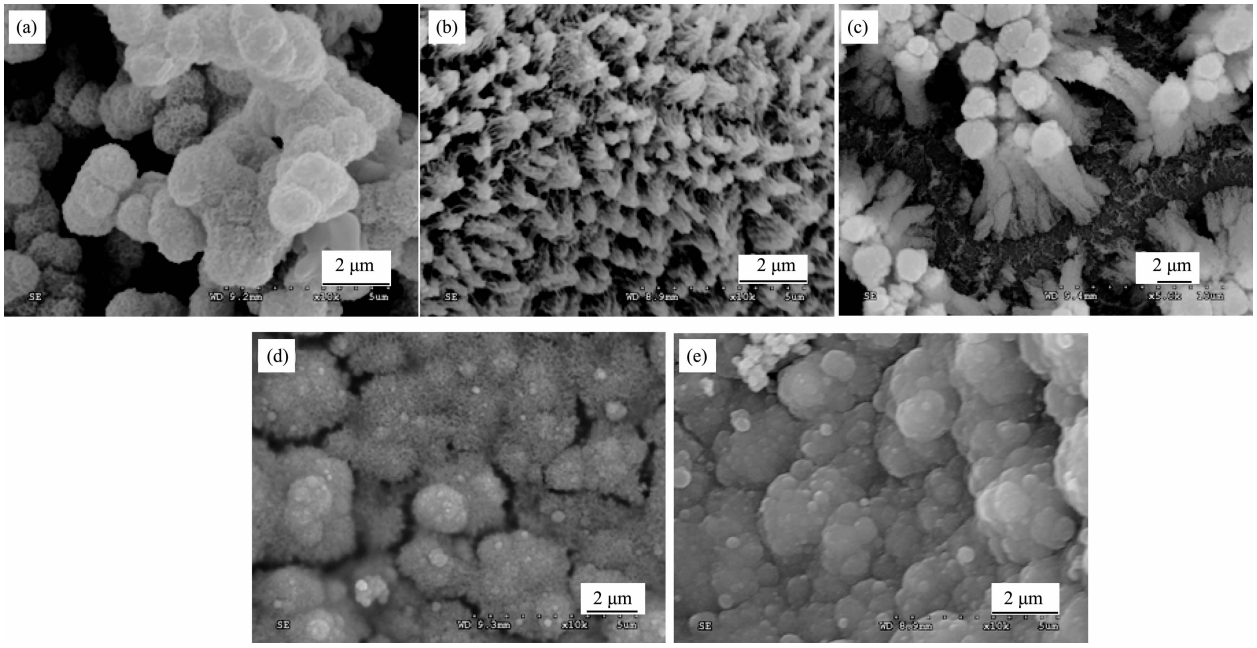

(a) 0, (b) 3.0, (c) 6.0, (d) 9.0 and (e) 12.0

Fig.5 SEM images of the products deposited at −0.6 V for 1 000 s in different pH value electrolytes

like fibers in 500~1 000 nm with straight orientation. When the pH value of the electrolyte is 6.0, the morphology of the products (Fig.5c) is bundles of microfibers with microparticles on the top. In alkaline solutions, the morphologies of the deposits are remarkably different. As depicted in Fig.5d, in a pH= 9.0 electrolyte, the deposits show agglomerated small particles, and there are short fibers of 20~30 nm in diameter in the particles surface. These deposits are denser than that in acidic solutions. When the pH value becomes 12.0, the short fibers on the particles disappear, and the particles surface becomes more slippery, as shown in Fig.5e. The XRD pattern shown in Fig.6 indicates that the product prepared in pH value of 0 (curve a) is a mixture of dominating cryptomelane-type potassium manganese oxide and less of birnessite-type potassium manganese oxide, and mainly birnessite-type potassium manganese oxide at pH value of 12.0 (curve b). This result is similar to that of Fig.1, which confirms the pH value dependence procedure in the deposition of potassium manganese oxides. SEM and XRD results show that the component and morphology of the prepared potassium manganese oxides can be controlled by adjusting the acidity of solutions and/or deposition time.

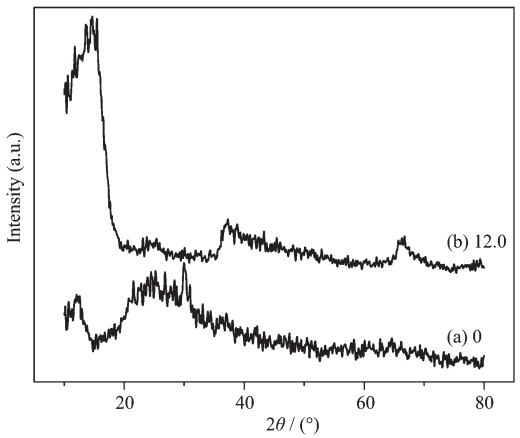

Fig.6 XRD patterns of the samples deposited at −0.6 V for 1 000 s in different pH value electrolytes

The role of depositing potential was also investigated by SEM technique. When the deposition time is 1 000 s, irregular microparticles of 2.0~5.0 μm could be obtained at −0.8 V (Fig.7a). If the deposition potential increases to −0.3 V, the products are irregular fragments with double layered structure, microparticles on a film with thickness of about 1.5 μm as shown in Fig.7c. When the depositing potential is 0 V, the products are irregular and glazed (Fig.7d).

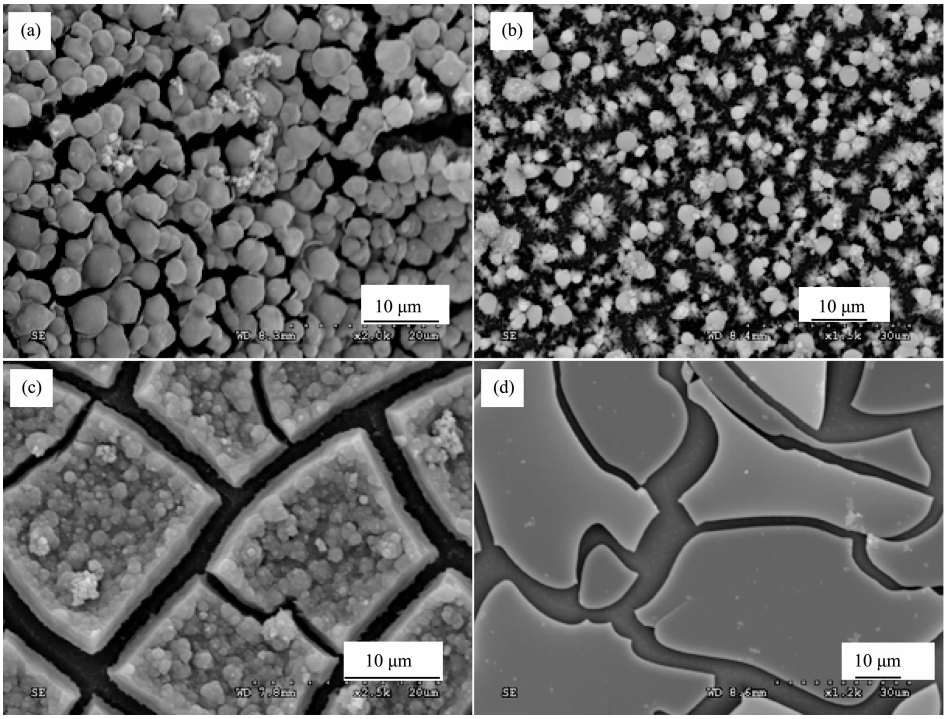

(a) −0.8 V, (b) −0.6 V, (c) −0.3 V, (d) 0 V

Fig.7　SEM images of the products deposited for 1 000 s at different potentials

2.4　Electrochemical properties

The electrochemical properties of the products deposited at −0.6 V for different time were investigated in 0.2 mol·L^{-1} K_2SO_4 solution. The potential range in CV was from 0.0 to 1.0 V and different scanning rates were taken from 2 to 200 mV·s^{-1}. Fig.8 shows the CV curves for the products deposited for 500, 3 000 and 6 000 s at 10 mV·s^{-1}, respectively, where the current is transferred into the current density of per unit mass of deposits. It can be seen that the specific capacitance of the products deposited for 500 s is higher than that of deposited for 3 000 and 6 000 s at the same scan rate. In addition, there is a cathodic peak at 0.42 V and an anodic peak at 0.69 V for products deposited for 500 s, correponding to the intercalation/deintercalation processes of cations. For the products deposited for 500 s, the voltammetric response on the positive sweep is nearly symmetrical to that on the following negative sweep, indicating good electrochemical reversibility of the electrode. As for the products deposited for 3 000 and 9 000 s, the CV curves show more components of resistance response, and the peaks of intercalation/deintercalation of cations are neglectable.

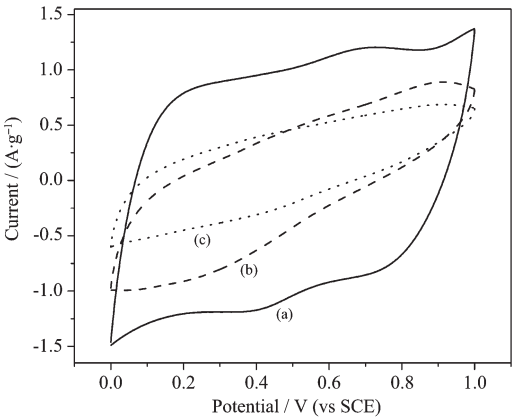

(a) 500, (b) 3 000, (c) 6 000 s

Fig.8　Cyclic voltammograms of the products deposited for different times in a 0.2 mol·L^{-1} K_2SO_4 solution at scan rate of 10 mV·s^{-1}

Fig.9 shows the relationship of SC value and scanning rates of the as-prepared potassium manganese oxides. The SC value can be estimated using half the integrated area of the CV curve to obtain the charge density, and then divided by the width of the potential window. At a low sweep rate of 2 mV·s^{-1}, the calculated SCs are 119.4, 99.5 and 109.0 F·g^{-1} corresponding to the products deposited for 500, 3 000 and 6 000 s,

respectively. However, at a scan rate of 200 mV·s^{-1}, the calculated SCs values are 7.7, 7.6 and 7.5 F·g^{-1}, respectively. As shown in Fig.9, the reduction rate of SCs is increased with deposition time, which could be attributed to the low conductivity and/or the electrolyte diffusion limitations in the potassium manganese oxides.

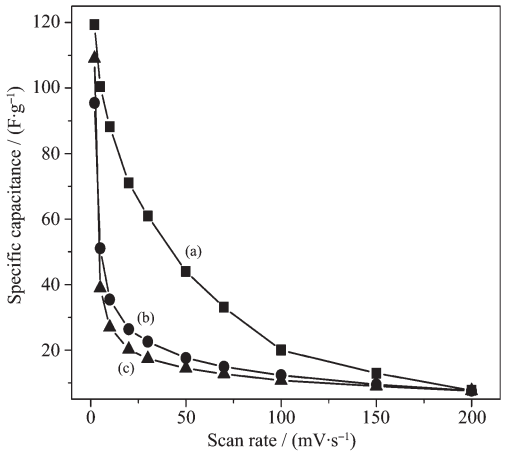

(a) 500, (b) 3 000, (c) 6 000 s

Fig.9 Effect of scan rate on the specific capacitance of the products deposited for different times in 0.2 mol·L^{-1} K_2SO_4

In order to further understand the influence of scanning rates on SC, voltammetric charges have been determined as a function of scan rates. Trasatti and his co-workers firstly propounded to discriminate the "inner" and "outer" charges of electrode materials[50]. The whole surface of the electrode could be divided into "inner" surface (which is more difficult to access by the charge compensating ions) and "outer" surface (which is straightforwardly accessible to the charge compensating ions). The fast scanning rate will lead to the H^+ or alkali metal cations reaching only the "outer" surface of the electrode, the extrapolation of q to $v=\infty$ ($v^{-1/2}=0$) shows the "outer" charge (q_O), which is the charge on the most accessible active surface. The dependence of voltammetric charge (q) on the inverse of the square root of scanning rate ($v^{-1/2}$) is shown in Fig.10a. Fig.10b denotes the inverse of the voltammetric charge (q^{-1}) on the square root of sweep rate ($v^{1/2}$), in which the extrapolation of q^{-1} to $v^{1/2}$ gives the total charge (q_T), that is, the charge related to the whole active surface. The estimated charges at very low (q_T) and high scan rates (q_O) for the samples prepared at various deposition times are summarized in Table 1. It can be seen that the charge of the products deposited for 500 s at very low scan rate is higher than that of 3 000 and 6 000 s, and the value is 305.8 C·g^{-1}, which is primarily attributed to the thin films advantage in mass transportation and

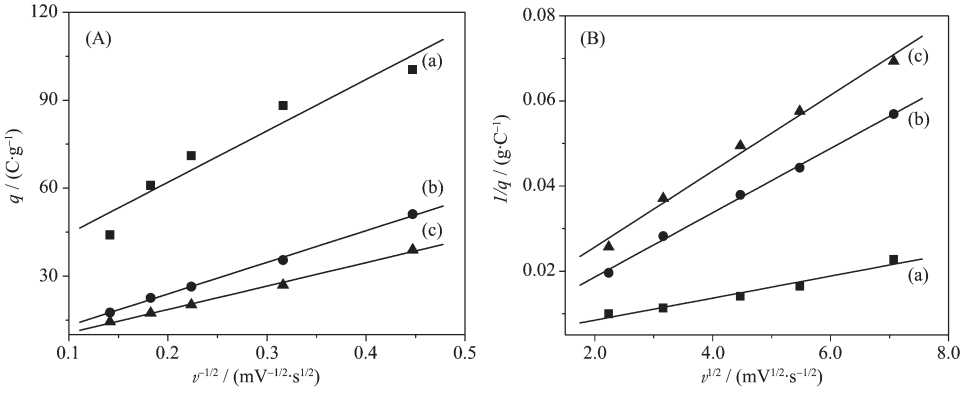

Fig.10 Variation of voltammetric charge density (q) with respect to scan rate (v): (A) q vs $v^{-1/2}$ and (B) $1/q$ vs $v^{1/2}$ Line (a), (b) and (c) representing the deposition time to be 500, 3 000 and 6 000 s

Table 1 Estimated charge density (C·g^{-1}) at very low and very high scan rates for all samples deposited for different times

Deposition time / s	q_O / (C·g^{-1})	q_T / (C·g^{-1})
500	27.0	305.8
3 000	2.3	288.2
6 000	2.7	128.2

facilitating the intercalation and deintercalation of cations. The relative low SC values of the products deposited for 3 000 and 6 000 s reveal that most surfaces of the products are inaccessible for cations and their higher resistance characters. Therefore, large decrease is expected in specific capacitance at higher scan rates.

The prepared materials were subjected to galvanostatic charge/discharge cycling between 0 and 1.0 V in 0.2 mol·L^{-1} K_2SO_4 solution at a current density of 0.5 A·g^{-1}. Typical curves of potential variation during the third cycle are shown in Fig.11. For products deposited for 500 s, the almost linear charge/discharge curve and equivalent charge and discharge time indicates a good capacitive behavior. When the deposition time extends to 3 000 and 6 000 s, the charge/discharge curves deviate from the linearity, and the observed IR drop increases, which mean that the conductivity of the products decreases with the deposition time, and it is consistent with the CV results. Along with the increase of deposition time, the charging time of the products is longer than discharging time, especially in the first and second cycles (shown in the inset in Fig.11), which implies the reversibility of the prepared potassium manganese oxides is dropping with deposition time. The average SC values in the third cycle are 114.4, 35.4 and 22.7 F·g^{-1}, respectively,

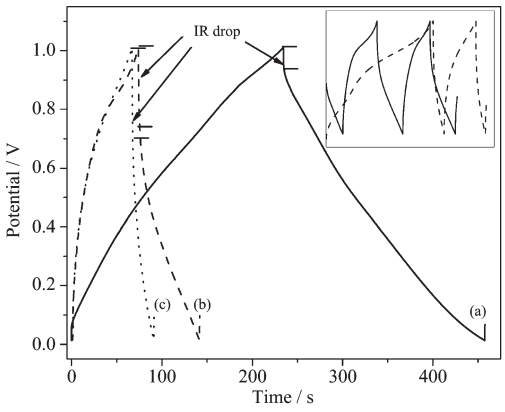

Fig.11 Third charge/discharge cycle of the products measured at 0.5 A·g^{-1} in 0.2 mol·L^{-1} K_2SO_4 for different deposition time: (a) 500, (b) 3 000 and (c) 6 000 s, respectively; Inset is the first and second charge/discharge cycles of the products deposited for 3 000 s (solid line) and 6 000 s (dashed line)

which is close to that of calculated ones from the CV studies at 5 mV·s^{-1}.

3 Conclusion

Potas sium manganese oxides were prepared by cathodic reduction of $KMnO_4$ solutions. Experimental results show that the deposits component is altering with the preparing factors such as applied potential, deposition time and the electrolytes acidity. The morphology and size of the products could be also controlled through adjusting the deposition parameters. The deposition potassium manganese oxide from aqueous $KMnO_4$ is a pH value dependent procedure. The specific capacitance of the products deposited for 500 s is higher than that of 3 000 and 6 000 s due to the facilitating of intercalation and deintercalation of cations. At a scan rate of 2 mV·s^{-1} in 0.2 mol·L^{-1} K_2SO_4 aqueous electrolyte, the specific capacitances of products are 119.4, 99.5 and 109.0 F·g^{-1} corresponding to the deposition time of 500, 3 000 and 6 000 s, respectively. In addition, the dissimilar cyclic voltammetry response, the different IR drops and the different charge/discharge times indicate the reversibility and performance of these potassium manganese oxides as capacitor materials.

References:

[1] Conway B E. *Electrochemical Supercapacitors*. New York: Kluwer Academic Publishers, **1999**.

[2] Lee H Y, Goodenough J B. *J. Solid State Chem.*, **1999**,**144**: 220-223

[3] Pang S C, Anderson M A, Chapman T W. *J. Electrochem. Soc.*, **2000**,**147**:444-450

[4] Pang S C, Anderson M A. *J. Mater. Res.*, **2000**,**15**:2096-2106

[5] Ma S B, Nam K W, Yoon W S, et al. *J. Power Sources*, **2008**, **178**:483-489

[6] Hsieh Y C, Lee K T, Lin Y P, et al. *J. Power Sources*, **2008**, **177**:660-664

[7] Xu C J, Li B H, Du H D, et al. *J. Power Sources*, **2008**,**180**: 664-670

[8] Abou-El-Sherbini K S, Askar M H. *J. Solid State Electrochem.*, **2003**,**7**:435-441

[9] Golden D C, Chen C C, Dixon J B. *Science*, **1986**,**231**:717-719

[10]Feng Q, Liu L, Yanagisawa K J. *Mater. Sci. Lett.*, **2000**,**19**:1567-1570
[11]Franger S, Bach S, Pereira-Ramos J P, et al. *J. Electrochem. Soc.*, **2000**,**147**:3226-3230
[12]Yang D S, Wang M K. *Chem. Mater.*, **2001**,**13**:2589-2594
[13]Cai J, Liu J, Suib S L. *Chem. Mater.*, **2002**,**14**:2071-2077
[14]Prieto O, Del Arco M, Rives V. *J. Mater. Scienc*, **2003**,**38**:2815-2824
[15]Yang L X, Zhu Y J, Cheng G F. *Mater. Res. Bull.*, **2007**,**42**:159-164
[16]Gaillot A C, Drits V A, Manceau A, et al. *Micropor. Mesopor. Mater.*, **2007**,98:267-282
[17]Liu Z H, Kang L, Ooi K, et al. *J. Colloid Interface Sci.*, **2005**, **285**:239-246
[18]Feng Q, Liu L, Yanagisawa K, et al. *Mater. Sci. Lett.*, **2000**, **19**:1567-1570
[19]Morales J, Sanchez L, Bach S, et al. *Mater. Lett.*, **2002**,**56**:653-659
[20]Gaillot A C, Lanson B, Drits V A. *Chem. Mater.*, **2005**,**17**:2959-2975
[21]Franger S, Bach S, Farcy J, et al. *J. Power Sources*, **2002**, **109**:262-275
[22]Julien C, Massot M, Baddour-Hadjean R, et al. *Solid State Ionics*, **2003**,**159**:345-356
[23]Bach S, Pereira-Ramos J P, Willmann P. *Electrochim. Acta*, **2006**,**52**:504-510
[24]Ching S, Welch E J, Hughes S M, et al. *Chem. Mater.*, **2002**, **14**:1292-1299
[25]Ching S, Hughes S M, Gray T P, et al. *Micropor. Mesopor. Mater.*, **2004**,**76**:41-49
[26]Chang J K, Tsai W T. *J. Appl. Electrochem.*, **2004**,**34**:953-961
[27]Hu C C, Tsou T W. *Electrochim. Acta*, **2002**,**47**:3523-3532
[28]Hu C C, Tsou T W. *J. Power Sources*, **2003**,**115**:179-186
[29]Chang J K, Chen Y L, Tsai W T. *J. Power Sources*, **2004**,**135**:344-353
[30]Broughton J N, Brett M J. *Electrochim. Acta*, **2005**,**50**:4814-4819
[31]Nagarajan N, Humadi H, Zhitomirsky I. *Electrochim. Acta*, **2006**,**51**:3039-3045
[32]Nagarajan N, Cheong M, Zhitomirsky I. *Mater. Chem. Phys.*, **2007**,**103**:47-53
[33]Liu D, Garcia B B, Zhang Q, et al. *Adv. Funct. Mater.*, **2009**, **19**:1015-1023
[34]Wei J, Nagarajan N, Zhitomirsky I. *J. Mater. Process. Tech.*, **2007**,**186**:356-361
[35]Wang Y, Liu H, Sun X, et al. *Scripta Mater.*, **2009**,**61**:1079-1082
[36]Fan Z, Chen J, Zhang B, et al. *Diam. Relat. Mater.*, **2008**,**17**:1943-1948
[37]Li J, Zhitomirsky I. *Colloids Surfaces A*, **2009**,**348**:248-253
[38]Jacob G M, Zhitomirsky I. *Appl. Surf. Sci.*, **2008**,**254**:6671-6676
[39]Zhitomirsky I, Cheong M, Wei J. *JOM*, **2007**,**59**:66-69
[40]Wei J, Zhitomirsky I. *Surf. Eng.*, **2008**,**24**:40-46
[41]Cheong M, Zhitomirsky I. *Surf. Eng.*, **2009**,**25**:346-352
[42]Jacob G M, Zhitomirsky I. *J. Nano Res.*, **2009**,**7**:87-92
[43]Toupin M, Brousse T, Bélanger D. *Chem. Mater.*, **2002**,**14**:3946-3952
[44]Chigane M, Ishikawa M. *J. Electrochem. Soc.*, **2000**,**147**:2246-2251
[45]Gao T, Norby P, Krumeich F, et al. *J. Phys. Chem. C*, **2010**, **114**:922-928
[46]Tan B J, Klabunde B J, Sherwood P M A. *J. Am. Chem. Soc.*, **1991**,**113**:855-861
[47]Hu C C, Wang C C. *J. Electrochem. Soc.*, **2003**,**150**:A1079-A1084
[48]Banerjee D, Nesbitt H W. *Geochim. Cosmochim. Acta*, **1999**, **63**:3025-3038
[49]Chigane M, Ishikawa M, Izaki M. *J. Electrochem. Soc.*, **2001**, **148**:D96-D101
[50]Ardizzone S, Frengonara G, Trasatti S. *Electrochim. Acta*, **1990**,**35**:263-267